



Cite this: *Soft Matter*, 2020, 16, 2128

Unification of lower and upper critical solution temperature phase behavior of globular protein solutions in the presence of multivalent cations†

Nafisa Begam,^{id}*^a Olga Matsarskaia,^{id}‡^a Michael Sztucki,^b Fajun Zhang^{id}*^a and Frank Schreiber^{id}^a

In globular protein systems, upper critical solution temperature (UCST) behavior is common, but lower critical solution temperature (LCST) phase transitions are rare. In addition, the temperature sensitivity of such systems is usually difficult to tune. Here we demonstrate that the charge state of globular proteins in aqueous solutions can alter their temperature-dependent phase behavior. We show a universal way to tune the effective protein interactions and induce both UCST and LCST-type transitions in the system using trivalent salts. We provide a phase diagram identifying LCST and UCST regimes as a function of protein and salt concentrations. We further propose a model based on an entropy-driven cation binding mechanism to explain the experimental observations.

Received 26th November 2019,
Accepted 27th January 2020

DOI: 10.1039/c9sm02329a

rsc.li/soft-matter-journal

1 Introduction

Understanding protein phase behavior is important in several areas such as medicine or biotechnology. As an example, the formation of a dense phase after protein phase separation underlies several human pathologies. A case in point is sickle-cell anemia, where phase separation plays a crucial role in the deformation of erythrocytes.¹ In the context of material science, protein engineering opens up new opportunities for the development of biomaterials. Stimulus-triggered changes in water solubility causing phase separation of protein solutions are important aspects in this field.^{2–4} Such stimuli include temperature, pH, and ionic strength.^{4–8} Therefore, studying the influence of these parameters can help elucidate the phase behavior of protein solutions and propel the understanding of biological processes including transport, catalysis, and supramolecular organization of cellular tissues.^{9,10} In particular, studies of thermoresponsive proteins drive innovations in their application as scaffolds for bioactive compounds and drug delivery vehicles.^{11–13}

In the case of synthetic polymers, thermoresponsivity has been shown to be able to lead to phase separation above (lower critical solution temperature, LCST)¹⁴ as well as below a critical temperature (upper critical solution temperature, UCST)^{15,16}

depending on the exact balance of the interaction energies and entropic contributions. Importantly, some polymers exhibit tunable phase transitions with both UCST and LCST.^{17–19} The classical Flory–Huggins theory has successfully described the UCST phase behavior based on the framework of entropy and enthalpy of mixing/demixing.^{20,21} On the other hand, the gain in entropy caused by a release of bound water molecules was described as a thermodynamic driving force behind LCST.^{22,23} Theoretical works predict that the enthalpy of mixing changes from positive near UCST to negative near LCST.^{24,25} In addition, the volume change upon mixing is negative near LCST, and either negative or positive near UCST.^{24,25} In the case of block-copolymers, the behavior was found to be strongly dependent on the fraction of copolymers. Wu *et al.* have shown a transition from an LCST to a UCST by changing the chain length of poly(vinyl alcohol) grafted on poly(*p*-dioxanone).¹⁸ Zhu *et al.* designed poly(2-vinyl-4,4-dimethylazlactone) with either UCST or LCST or both by making the lactones react with sulfo-propylbetaine (SPB) amine, sulfo-butylbetaine (SBB) amine, tetrahydrofurfurylamine (THF amine) and other molecules.²⁶ In addition, LCST and UCST phase behavior determined by the charge state of the side chains of polypeptides has been studied.²⁷ Similarly, the existence of both UCST and LCST is well known in resilin elastic proteins due to three competing factors: the attractive protein–protein interaction, the formation of hydrogen bonds and the entropy of mixing.^{22,28,29} In line with this concept, Quiroz *et al.* demonstrated that the amino acid sequence of elastins controls the phase transition and designed amino acid sequences encoding tunable LCST and UCST.^{30,31} However, such investigations on globular proteins have not

^a Institut für Angewandte Physik, Universität Tübingen, 72076 Tübingen, Germany.
E-mail: nafisa.phy@gmail.com, fajun.zhang@uni-tuebingen.de

^b ESRF – The European Synchrotron, 71 Avenue des Martyrs, 38000 Grenoble, France

† Electronic supplementary information (ESI) available. See DOI: 10.1039/c9sm02329a

‡ Present address: Institut Laue-Langevin, 71 Avenue des Martyrs, 38042 Grenoble, France.

been reported so far. While UCST is common in globular proteins,^{5,32–36} LCST is rare.^{7,37,38} In addition, one of the main bottlenecks is that the temperature-sensitive properties of proteins are rarely tunable. Along these lines, a broader goal is to be able to recognize the conditions that lead to LCST and/or UCST in a globular protein system.

The globular proteins β -lactoglobulin (BLG) and bovine serum albumin (BSA) have been reported to exhibit re-entrant condensation phase behavior in the presence of yttrium chloride (YCl_3).^{7,36} The phase diagram of these systems indicates two critical concentrations of YCl_3 , c^* and c^{**} , within which such a phase transition occurs. BLG- YCl_3 showed a usual UCST phase behavior near c^{**} .³⁶ On the other hand, BSA has been proven to show an unusual LCST phase behavior with liquid–liquid phase separation (LLPS) for YCl_3 concentrations between c^* and c^{**} .⁷ These studies give rise to the question whether a particular system, consisting of globular proteins with their different configurations and inhomogeneous surface charges, can exhibit both LCST and UCST.

In order to contribute to the answer of the above question, here we show a universal way to tune the interactions and hence UCST and LCST behavior using trivalent salts in aqueous solutions of the proteins BLG and BSA. We observe the existence of both transitions in one system over a wide range of protein concentrations. This study suggests that an entropy-driven cation binding to the protein surface selectively leads to either UCST or LCST. We establish a phase diagram identifying both LCST and UCST regimes as a function of protein and salt concentrations for the protein BLG. Our findings contribute to the physical understanding of protein phase behavior in response to the temperature in aqueous environments.

2 Experimental details

BLG (product no. L3908, Merck, Germany) from bovine milk and BSA (product no. A7906, Merck, Germany) from bovine blood were used for this study as received. BLG is a globular protein with a molecular weight of 18.4 kDa and contains 162 amino acids. BSA is also globular with an approximately ellipsoidal shape and consists 583 amino acids (molecular weight of 66.5 kDa). In the following we will refer to the protein concentration as c_p . BLG was dissolved in de-gassed de-ionized H_2O (resistivity of 18.2 M Ω cm, Milli-Q, Merck, Germany) and left at 4 °C for 1 day to homogenize the solution. The concentration of the solution was determined using ultraviolet-visible (UV-Vis) absorption spectroscopy (absorption at 280 nm).³⁷ YCl_3 (product no. 451363, Merck, Germany) was dissolved in de-gassed H_2O , equilibrated at room temperature for approximately 12 h and filtered using 0.2 μm membrane filters (Whatman Cellulose Filters, Merck, Germany). Samples were made by mixing YCl_3 and BLG solutions at room temperature. The concentration of BLG, c_p (in mg ml^{-1}), in the final solutions was varied from 3.5 to 40 mg ml^{-1} . The same procedure was followed to make BSA- YCl_3 solutions in water (prepared at room temperature). The extinction coefficients of the BLG and BSA solutions used for the concentration determinations are

0.966 and 0.667 $\text{mg}^{-1} \text{ ml cm}^{-1}$, respectively (ref. 36 and 37). In the final solutions, c_p was kept constant at 100 mg ml^{-1} and the concentration of YCl_3 , c_s (mM) was varied for BSA- YCl_3 solutions. The samples that were turbid at room temperature due to phase separation in Regime II were kept at 21 °C for a short time followed by centrifugation and only the supernatants were used for further measurements.⁷

To determine the transition temperatures (T_{trans}) of the samples, we performed turbidity measurements using a UV-Vis spectrometer equipped with a water bath for temperature control (Haake A10B and SC 150, Thermo Fisher Scientific Inc., Germany) by measuring the optical turbidity of the samples over a wavelength range of 400 to 800 nm as a function of temperature. The sample was heated/cooled at a rate of 0.5 °C minute^{-1} . To identify the condensed state we used an optical microscope (AxioScope A1 from Carl Zeiss, Germany) with a 50 \times magnification. A heating/cooling stage (Linkam Scientific Instruments Ltd, UK) was used to control the sample temperature with an accuracy of 0.1 °C using liquid nitrogen flow.

To quantify the protein interactions in the BLG- YCl_3 and BSA- YCl_3 systems, we have performed small angle X-ray scattering (SAXS) using a laboratory X-ray source (Xeuss 2.0, Xenocs, France, with $\lambda = 1.54 \text{ \AA}$) as well as beamline ID02 of the ESRF (Grenoble, France, with $\lambda = 0.998 \text{ \AA}$)³⁹ on these samples as a function of temperature. The protein solutions were filled into quartz capillary tubes with a diameter of 1.5 mm (and of 1 mm diameter in the case of ID02) and mounted on the sample stage equipped with a heating stage and a temperature controller (Linkam Scientific Instruments Ltd, UK). The sample to detector distance was 30.7 m at beamline ID02, and 1 m in the laboratory X-ray setup. In this configuration, the q range available, where q is the wave vector transfer ($= \frac{4\pi \sin \theta}{\lambda}$, with 2θ being the scattering angle) is 1×10^{-4} to $7 \times 10^{-3} \text{ \AA}^{-1}$ at ID02 and 0.007 to 0.23 \AA^{-1} at the laboratory X-ray setup.

3 Results

3.1 Temperature sensitivity of BLG- YCl_3

We first present an example experiment to demonstrate the existence of both LCST and UCST behavior in the BLG- YCl_3 system by varying c_s . Fig. 1(a and b) show that the supernatant of the solution with $c_p = 40 \text{ mg ml}^{-1}$ and $c_s = 10 \text{ mM}$ (the left sample) is clear in a hot water bath but turbid in a cold bath. Thus, it shows a UCST. This behavior of BLG- YCl_3 systems was observed earlier.³⁶ Nevertheless, the supernatant of a solution with $c_p = 40 \text{ mg ml}^{-1}$ and a low $c_s = 4 \text{ mM}$ (the right sample) is turbid at high temperature and clear at a low temperature, thus exhibiting LCST.^{7,37} Both transitions are observed to be reversible. A globular protein solution showing both transitions has rarely been observed.³⁰ Our experiments clearly indicate that a globular protein solution can exhibit both LCST and UCST depending on c_s (see Video S1, ESI†).

We further investigated the samples using optical microscopy during the phase separation process. Micrographs for the BLG- YCl_3 samples with $c_p = 40 \text{ mg ml}^{-1}$ and $c_s = 4 \text{ mM}$ (LCST)

BLG = 40 mg/ml, $\text{YCl}_3 = 10$ (left) and 4 mM (right)

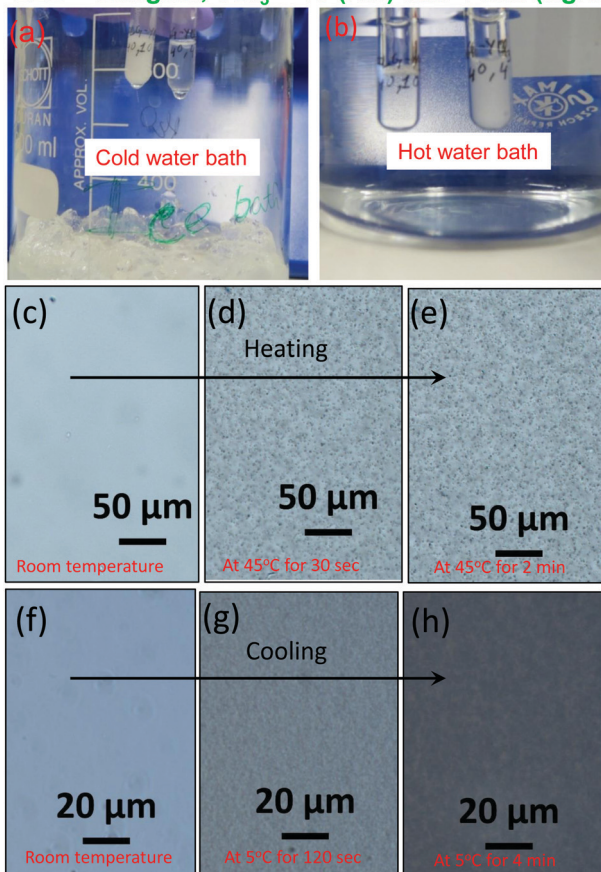


Fig. 1 Experimental demonstration of temperature sensitivity of the BLG- YCl_3 solutions using cold and hot water baths. The solution (a) with low c_s (4 mM, the right sample in both (a) and (b)) becomes turbid at a high temperature (LCST) and the solution (b) with high c_s (10 mM, the left sample in both (a) and (b)) becomes turbid at a low temperature (UCST), thus showing a rather unusual combination of both types of critical temperatures in globular proteins. Light micrographs of the uniform solution (c), the sample at 45 °C for 30 s (d) and after 2 min (e) for the sample with LCST behavior, and micrographs for the sample with UCST behavior when uniform (f), at 5 °C for 120 s (g), and after 4 min (h).

and 10 mM (UCST) are shown in Fig. 1(c-e) and (f-h), respectively, at different times during the phase separation. In both cases of LCST and UCST, the dense domains are initially formed on heating above or cooling below the transition temperatures. However, the domains do not continue to grow as is expected for an LLPS (see Videos S2 for LCST and S3 for UCST, ESI†). The domain size reaches a certain value and then remains almost constant with time. After several hours (~ 3 –4 hours) the sample shows a white precipitate which starts to crystallize upon further waiting (over a time span of ~ 8 –12 hours).

Next, we present systematic temperature-dependent turbidity-based experimental results indicating both UCST and LCST for two c_p values in a broad range of c_s . The turbidity of the solution, averaged over the entire wavelength range, is plotted (see Fig. 2) as a function of temperature. Fig. 2(a) shows a sharp transition from clear to turbid on heating above a critical temperature for $c_p = 15 \text{ mg ml}^{-1}$ and c_s ranging from 1.3 to 1.8 mM indicating a

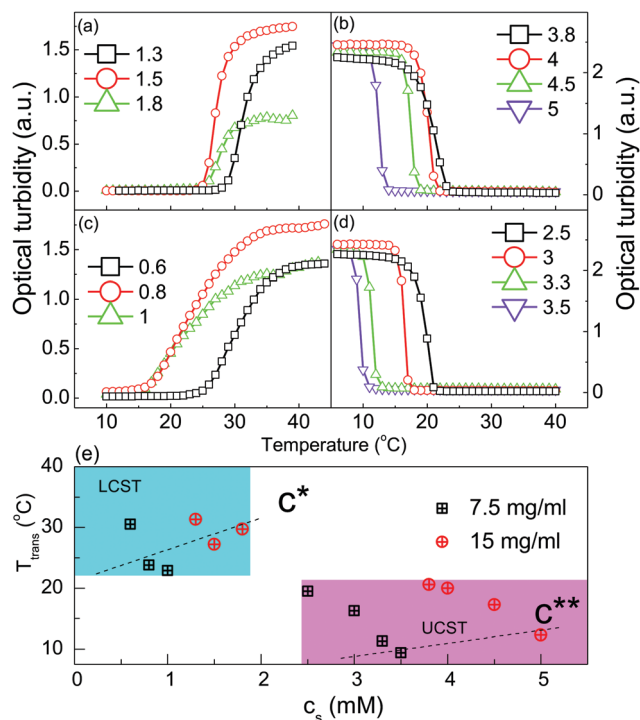


Fig. 2 Optical turbidity as a function of temperature to determine the phase behavior and transition temperatures for BLG- YCl_3 systems with (a and b) $c_p = 15 \text{ mg ml}^{-1}$ and varying c_s (in mM) as indicated in the legends, and (c and d) $c_p = 7.5 \text{ mg ml}^{-1}$ (lines are a guide to the eye). Part (e) shows a summary of T_{trans} as a function of c_s in the BLG- YCl_3 system at two different c_p (7.5 and 15 mg ml^{-1}) indicating an overall decrease in T_{trans} with increasing c_s . The two phase regime is indicated by the area between the two dashed lines.

typical LCST behavior. Fig. 2(b) illustrates a different behavior with increasing c_s (for the same c_p of 15 mg ml^{-1}). Here a sharp transition from clear to turbid on cooling below a critical temperature is observed (UCST-type behavior). Similarly, both LCST-type (at low c_s) and UCST-type (at high c_s) behaviors are observed for samples with $c_p = 7.5 \text{ mg ml}^{-1}$ as we can see in Fig. 2(c and d). Such an observation of an LCST behavior at low c_s and a UCST behavior at high c_s provides a hint that protein phase behavior can be manipulated by tuning the charge state of the protein solution mediated by the salt used. The inflection point of the turbidity vs. temperature plot corresponds to the transition temperature. Fig. 2(a-d) also indicates that T_{trans} shifts to lower values with increasing c_s . In addition, in the case of UCST, the transition seems to be sharper than that in the case of LCST. T_{trans} values of all samples were determined from the temperature dependent turbidity data by fitting them with a sigmoidal function. T_{trans} values for two different c_p values are summarized in Fig. 2e. An overall decrease of T_{trans} with increasing c_p is observed for both UCST³⁶ (shown on a magenta background) and LCST (shown on a cyan background) which is consistent with previous reports³⁶ (this is discussed in Section 4).

In order to study the interactions of the proteins, we performed SAXS with varying temperature on the supernatant of a sample with c_p of 6.6 mg ml^{-1} and c_s of 2.5 mM exhibiting UCST. The sample was cooled down from 21 to 7 °C and then

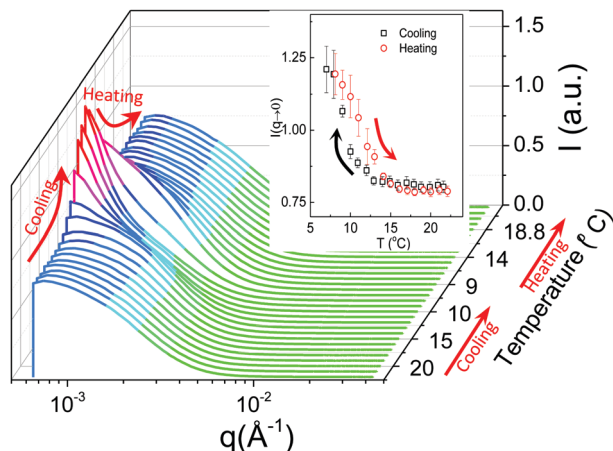


Fig. 3 SAXS intensity profiles collected during a temperature cycle (decrease from 21–7 °C and then increase from 7–21 °C) on BLG-YCl₃ with $c_p = 6.6 \text{ mg ml}^{-1}$ and $c_s = 2.5 \text{ mM}$ (UCST behavior). The data shows a reversibility of the cooling-induced structural change when the sample is heated back to 21 °C. The colorcode added here is to emphasize the intensity change in different q regions. The inset shows a decrease in $I(q \rightarrow 0)$ with increasing temperature reflecting a UCST phase transition.

heated to 21 °C again. The corresponding scattering intensity profiles, $I(q)$ are shown in Fig. 3. Water scattering was used for the background correction. As can be seen from Fig. 3, the intensity at low q ($I(q \rightarrow 0)$) significantly increases at temperatures below 13 °C which is indicative of a reduction in surface charge-induced repulsion and dominating attractive interactions.⁴⁰ At this stage, the solution starts to phase-separate. The intensity reverts back to the previous value when the sample is heated back to ~21 °C, implying a reversible phase separation.

To investigate the effective interactions we have plotted $I(q \rightarrow 0)$ as a function of temperature (inset of Fig. 3). Here we have taken the average intensity of the 1st to the 5th data points (q range corresponds to 6.4×10^{-4} – $9.8 \times 10^{-4} \text{ \AA}^{-1}$) and plotted this value as a function of temperature. In the regime of the phase diagram without LLPS, it has been shown, for a similar protein-trivalent salt system, that the inverse of $I(q \rightarrow 0)$ exhibits the same behavior as the second virial coefficient which is a measure of the strength of attraction/repulsion.^{41,42} In the current study, $I(q \rightarrow 0)$ increases when the sample is cooled from 21 to 7 °C (Fig. 3). This indicates an increase in protein–protein attraction.^{40,43} In our case, such an increase in protein–protein attraction with decreasing temperature leads to the phase separation observed at low temperatures (UCST). An estimation of the reduced second virial coefficient, B_2/B_2^{HS} from the SAXS data using a sticky hard sphere model (SHS) combined with an ellipsoidal form factor indicates a similar increase in attraction with decreasing temperature (Fig. S2 in the ESI†).

Based on all BLG samples investigated over a large range of c_p and corresponding c_s , the overall phase behavior is summarized in Fig. 4 in a c_s – c_p diagram. A diagram showing three distinct regimes of phase behavior of the BLG system at room temperature divided by c^* and c^{**} has been reported earlier.³⁶ Herein, we identify the regimes with different thermal responsivities of the BLG solutions in a similar phase diagram. The closed symbols (high c_s) indicate

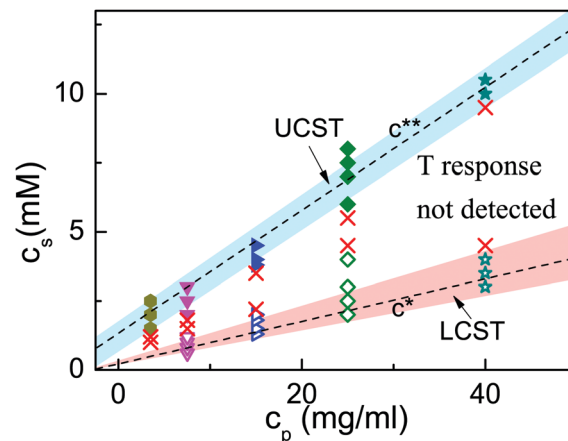


Fig. 4 c_s – c_p phase diagram showing the LCST (open symbols) and UCST (close symbols) regimes. The red cross symbols represent the samples that do not exhibit any temperature sensitivity within the temperature range investigated (0 to 45 °C). The dashed lines represent the two critical c_s values of re-entrant condensation of these samples, c^* and c^{**} .^{36,40}

UCST and the open symbols (low c_s) indicate LCST phase transitions of the solutions. These two regimes of UCST and LCST are shaded in blue and pink, respectively. Interestingly, the intermediate regime (red crosses), where c_s is smaller than that in the UCST regime and higher than that in the LCST regime, does not seem to show any temperature sensitivity within the temperature range studied (0 to 45 °C). Moreover, we observe that the turbid samples (without centrifugation) in the condensed regime do not show pronounced thermo-responsivity, either. The turbid appearance does not become clear by heating beyond or cooling below any temperature within the temperature range of 0 to 45 °C. This behavior remains the same if the sample is prepared at low temperature. It is therefore possible that the as-prepared turbid samples, (in the condensed regime) have a transition temperature which is not inside the measurement temperature regime, or do not exhibit any thermo-responsivity.

The re-entrant phase behavior of this system observed between c^* and c^{**} has been understood in terms of a short-ranged attractive potential between the protein molecules where the range and strength of the attraction is tunable by varying the multivalent ions added to the solution.^{36,42,44} Our previous work showing a UCST behavior of BLG-YCl₃ near c^{**} indicated that the system behaves differently away from c^{**} (within the condensed regime).³⁶ Consistent with these findings, the current study also reveals a UCST phase behavior near c^{**} and an LCST phase behavior away from c^{**} (near c^*). Moreover, we observe that the LCST and UCST behaviors are not confined to the condensed regime. The LCST regime is extended below c^* and the UCST regime is extended above c^{**} which can be seen in Fig. 4.

3.2 Temperature sensitivity of BSA-YCl₃

We extended our investigation to another system, namely BSA-YCl₃. Our previous work has shown that this system exhibits a robust LCST behavior in a certain range of c_s .^{7,37,45} A similar behavior of BSA is observed in the present study as well, which

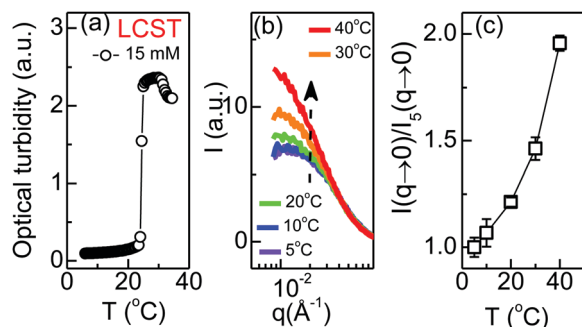


Fig. 5 (a) LCST phase transition for a BSA-YCl₃ sample with $c_s = 15$ mM and $c_p = 100$ mg ml⁻¹; the sample changes from clear to turbid with increasing temperature, (b) SAXS intensity profiles collected at different temperatures (legend indicates the temperatures) for a BSA-YCl₃ sample with $c_p = 100$ mg ml⁻¹ and $c_s = 10$ mM, and (c) $I(q \rightarrow 0)/I_5(q \rightarrow 0)$ as a function of temperature normalized to that at 5 °C ($I(q \rightarrow 0)/I_5(q \rightarrow 0)$) showing an increase with increasing temperature (lines are a guide to the eye). All of these measurements indicate LCST.

can be seen in Fig. 5(a) for $c_s = 15$ mM ($c_p = 100$ mg ml⁻¹) where the turbidity shows a sharp transition from clear to turbid on heating above the critical temperature, exhibiting an LCST-type behavior. Interestingly, at high c_s (~ 40 mM and above, *i.e.* near c^{**}), the solution does not show any macroscopic phase transition in the temperature range of 0–45 °C. In order to understand the underlying reason behind such a different temperature sensitivity with varying c_s , we have performed SAXS measurements on the solutions with a constant c_p (100 mg ml⁻¹) and at different c_s with varying temperature using our laboratory X-ray source.

SAXS intensity profiles as a function of q at different temperatures are shown in Fig. 5(b) for a sample with $c_s = 10$ mM ($c_s < c^*$). Water is used for background correction. The intensity at low q increases with increasing temperature (as indicated by the black arrow). An increase in $I(q \rightarrow 0)$ indicates stronger attraction^{40,43} at high temperatures. A slight increase of c_s to 15 mM results in a clear LCST transition (Fig. 5(a)) due to such an increase in attraction. The intensity at $q \rightarrow 0$ normalized to that at 5 °C ($I(q \rightarrow 0)/I_5(q \rightarrow 0)$) is shown in Fig. 5(c). In this setup (laboratory X-ray setup), the intensity was also averaged over the 1st to the 5th data points (corresponding q range is 0.008–0.0097 Å⁻¹).

Upon further increase of c_s (40 mM and above) the intensity at low q decreases with increasing temperature as indicated by the red arrow in Fig. 6(a). This behavior becomes more pronounced when c_s is increased (up to ~ 100 mM) (Fig. 6(b and c)). The results for high c_s for BSA samples ($c_p = 100$ mg ml⁻¹) are summarized in Fig. 6(d). A decrease in $(I(q \rightarrow 0)/I_5(q \rightarrow 0))$ with increasing temperature suggests that the inter-protein attraction decreases with increasing temperature, which is similar to the observation on the BLG-YCl₃ system in the UCST regime (inset of Fig. 3). B_2/B_2^{HS} obtained from the SAXS data using the SHS model in combination with an ellipsoidal form factor also supports the trends of $I(q \rightarrow 0)$ as a function of temperature in both cases of low and high c_s (see Fig. S3 in the ESI†). The inter-protein interaction seen by SAXS, thus, indicates the possibility of a UCST in BSA system at high c_s in addition to the LCST behavior

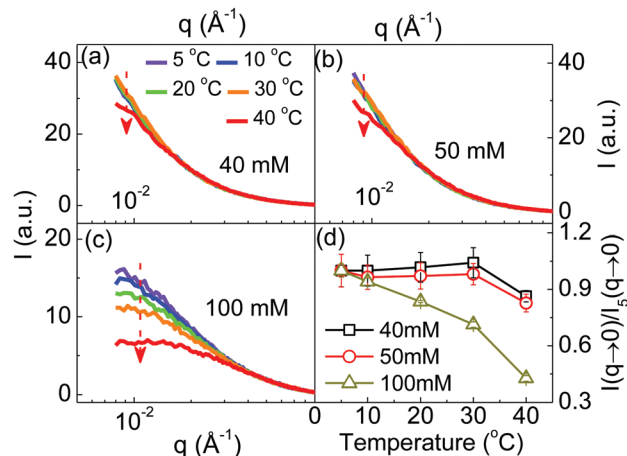


Fig. 6 SAXS intensity profiles for BSA-YCl₃ samples with $c_p = 100$ mg ml⁻¹ and (a) $c_s = 40$, (b) 50, (c) 100 mM, (d) $I(q \rightarrow 0)/I_5(q \rightarrow 0)$ as a function of temperature showing a decrease with increasing temperature for all the samples which is similar to that in the inset of Fig. 3 indicating a UCST-type behavior (as opposed to Fig. 5). Lines are a guide to the eye.

already reported earlier.^{7,37} We speculate that the attraction in the temperature range of 0–45 °C is possibly not strong enough to cause macroscopically visible UCST.

4 Discussion

UCST for globular protein solutions has been reported by several groups^{4,5} which can be described by a reduction of the system enthalpy dominating the entropy loss upon phase separation at low temperatures.^{46,47} However, LCST has rarely been observed in the case of globular proteins. Nevertheless, several reports have recently demonstrated a systematic LCST phase behavior in BSA-based systems.^{7,37,42,45} The mechanism behind such a phase behavior of globular protein systems was rationalized in ref. 7 and 48 using a concept of ion-activated attractive patches on the protein surface. Multidentate coordinative bonds between cations (*e.g.* Y³⁺ ions in the current study) and the carboxylic side chains of the protein surface eventually bridge the protein molecules. Such ion bridges between the protein molecules are analogous to attractive patches. This implies that such attractive patches activated by the ions can be tuned to alter the interactions and hence the phase behavior of globular proteins. Cation binding and bridging in the case of a negatively charged globular protein leads to a release of water molecules. This implies an entropy gain since the carboxylic binding sites of proteins as well as the cations are generally surrounded by hydration shells.^{49–51} Therefore, the temperature increase of the system is expected to enhance this bridging and make the protein–protein interaction stronger.⁷ The entropically favorable high bridging probability of the system at high temperatures causes phase separation upon heating and hence the system exhibits an LCST.

Yttrium binding sites present on protein surfaces, especially on the BLG surface (Fig. 7(a)), suggest that the LCST phase transition observed here at lower c_s in the BLG-YCl₃ system could be based on principles similar to the entropy-driven LCST

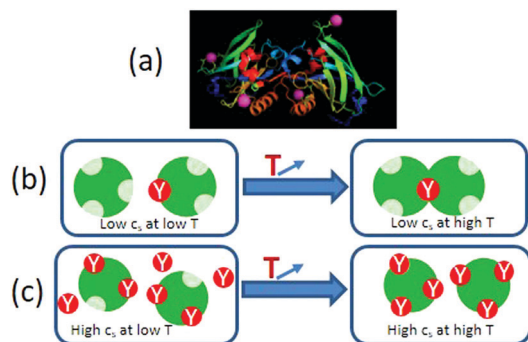


Fig. 7 (a) Molecular structure of BLG with the linking yttrium binding sites which are represented by magenta spheres (atomic coordinates have been taken from the Protein Data Bank with the code 3ph5). (b and c) Probability of ion binding and bridging at low (left panels) and high temperatures (right panels) demonstrating the case of LCST (b), and UCST (c) according to the ion-activated patchy particle model by Roosen-Runge *et al.*⁴⁸ Here the red circled Y represents the Y^{3+} ions and the green sphere represents the protein molecules (with three ion-activated attractive patches in this example). Note that the actual number of patches can vary in the real system.

as described above. This phenomenon is schematically shown in Fig. 7(b). The UCST phase transition observed could be hypothesized in terms of an over-crowding of ions in the solutions. In this case, the attractive patches are largely occupied by the cations and the fraction of unoccupied patches on the protein surface is much smaller compared to that at lower c_s , *i.e.*, with less ions. Therefore, it is expected that the probability of bridge formation between proteins is smaller compared to the binding of cations to the protein surface. This cation binding is enhanced with increasing temperature at high c_s , which makes the system more stable as illustrated schematically in Fig. 7(c). As a result the system exhibits a UCST phase transition at high c_s . Similarly, the presence of cation binding sites on BSA which is sequentially similar to the human serum albumin⁵² also manifests an indication of following a mechanism similar to BLG. At this point we can recall another finding presented above, *i.e.*, an increase in c_s leads to a decrease in T_{trans} . This can be understood as follows. In the case of LCST, an increase in c_s , meaning more ions, enhances ion-binding on the protein surfaces leading to an increasingly stronger protein-protein attraction. As a result the phase transition occurs at a lower temperature. Similarly, in the case of UCST, an increase in c_s tends to reduce the strength of attraction. Thus, the samples need to be cooled to lower temperatures to induce phase transition. Therefore, in both cases, an increase in c_s results in a decrease in T_{trans} .

The existence of closed-loop phase diagrams with both LCST and UCST has been demonstrated theoretically^{46,47,53} considering the competition between protein-protein interactions, entropy of mixing and hydration shells around proteins. Although the current study does not show a clear closed loop phase diagram, the results show the existence of both transitions in a single globular protein solution which can be tuned by c_s . This report thus provides experimental evidence of the presence of both critical temperatures in a same globular protein system exhibiting entropy-driven effects. In other words, the observation of both critical temperatures in the

same system leads to the unification of both phase transitions (UCST and LCST) by changing the concentration of multivalent ions in the solution.

5 Conclusions

In conclusion, we have shown a tunable LCST and UCST behavior of aqueous globular protein solutions by varying the salt concentrations. The BLG- YCl_3 solutions exhibit a pronounced LCST-type transition at low salt concentrations, and a UCST-type transition at high salt concentrations. On the other hand, the BSA- YCl_3 solutions show a clear LCST-LLPS behavior at low salt concentrations but no phase transition at high salt concentrations. However, an investigation of inter-protein interactions using SAXS provides an indication of UCST-type behavior of BSA- YCl_3 solutions at high salt concentrations. The transition temperatures are found to decrease with increasing salt concentration. In addition, our results show a reversibility of both phase transitions. Although the current study does not show a closed-loop phase diagram, possibly due to the fact that the measurement temperature range is limited by thermal denaturation of the proteins (at high temperature) and freezing of the solution (at low temperature), the results show the existence of both transitions in a single globular protein system. A phase diagram identifying LCST and UCST as a function of protein and salt concentrations for BLG- YCl_3 system is provided. We propose a model describing the phase behavior observed here in the framework of an entropy-driven phase transition in a patchy particle model system proposed previously in our group. Results of this study explore a new strategy of designing protein-based biomaterials with both LCST and UCST behavior.

Conflicts of interest

There are no conflicts of interest to declare.

Acknowledgements

The authors would like thank the European Synchrotron Radiation Facility for the allocation of beamtime at beamline ID02. This work was funded by the Deutsche Forschungsgemeinschaft (DFG). N. B. acknowledges the Alexander von Humboldt-Stiftung for a post-doctoral research fellowship, and O. M. thanks the Studienstiftung des Deutschen Volkes (German Academic Scholarship Foundation) for a PhD fellowship.

References

- O. Galkin, K. Chen, R. L. Nagel, R. E. Hirsch and P. G. Vekilov, *Proc. Natl. Acad. Sci. U. S. A.*, 2002, **99**, 8479–8483.
- P. Li, S. Banjade, H.-C. Cheng, S. Kim, B. Chen, L. Guo, M. Llaguno, J. V. Hollingsworth, D. S. Kind, S. F. Banani, P. S. Russo, Q.-X. Jiang, B. T. Nixon and M. K. Rosen, *Nature*, 2014, **483**, 336.
- P. G. Vekilov, *Soft Matter*, 2010, **6**, 5254–5272.

- 4 J. A. Thomson, P. Schurtenberger, G. M. Thurston and G. B. Benedek, *Proc. Natl. Acad. Sci. U. S. A.*, 1987, **84**, 7079–7083.
- 5 F. Cardinaux, T. Gibaud, A. Stradner and P. Schurtenberger, *Phys. Rev. Lett.*, 2007, **99**, 118301.
- 6 S. Bucciarelli, L. a. Casal-Dujat, C. De Michele, F. Sciortino, J. Dhont, J. Bergenholtz, B. Farago, P. Schurtenberger and A. Stradner, *J. Phys. Chem. Lett.*, 2015, **6**, 4470–4474.
- 7 O. Matsarskaia, M. K. Braun, F. Roosen-Runge, M. Wolf, F. Zhang, R. Roth and F. Schreiber, *J. Phys. Chem. B*, 2016, **120**, 7731–7736.
- 8 D. Durand, J. C. Gimel and T. Nicolai, *Phys. A*, 2002, **304**, 253–265.
- 9 W. R. Harris, *Coord. Chem. Rev.*, 1996, **149**, 347–365.
- 10 W. J. Ray and C. Bracker, *J. Cryst. Growth*, 1986, **76**, 562–576.
- 11 S. R. MacEwan and A. Chilkoti, *Nano Lett.*, 2012, **12**, 3322–3328.
- 12 J. A. MacKay, M. Chen, J. R. McDaniel, W. Liu, A. J. Simnick and A. Chilkoti, *Nat. Mater.*, 2009, **8**, 993.
- 13 D. E. Meyer and A. Chilkoti, *Biomacromolecules*, 2002, **3**, 357–367.
- 14 I. Dimitrov, B. Trzebicka, A. H. E. Müller, A. Dworak and C. B. Tsvetanov, *Prog. Polym. Sci.*, 2007, **32**, 1275–1343.
- 15 E. Karjalainen, V. Aseyev and H. Tenhu, *Macromolecules*, 2014, **47**, 7581–7587.
- 16 Q. Zhang and R. Hoogenboom, *Prog. Polym. Sci.*, 2015, **48**, 122–142.
- 17 S. Saeki, N. Kuwahara, S. Konno and M. Kaneko, *Macromolecules*, 1973, **6**, 246–250.
- 18 G. Wu, S.-C. Chen, Q. Zhan and Y.-Z. Wang, *Macromolecules*, 2011, **44**, 999–1008.
- 19 F. A. Plamper, M. Ballauff and A. H. E. Müller, *J. Am. Chem. Soc.*, 2007, **129**, 14538–14539.
- 20 P. J. Flory, *J. Chem. Phys.*, 1942, **10**, 51–61.
- 21 M. L. Huggins, *J. Chem. Phys.*, 1941, **9**, 440.
- 22 J. Li, R. Rajagopalan and J. Jiang, *J. Chem. Phys.*, 2008, **128**, 06B616.
- 23 H. G. Schild and D. A. Tirrell, *J. Phys. Chem.*, 1990, **94**, 4352–4356.
- 24 C. Baker, W. Brown, G. Gee, J. Rowlinson, D. Stubley and R. Yeadon, *Polymer*, 1962, **3**, 215–230.
- 25 E. A. Clark and J. E. G. Lipson, *Polymer*, 2012, **53**, 536–545.
- 26 Y. Zhu, R. Batchelor, A. B. Lowe and P. J. Roth, *Macromolecules*, 2016, **49**, 672–680.
- 27 C. Xing, Z. Shi, J. Tian, J. Sun and Z. Li, *Biomacromolecules*, 2018, **19**, 2109–2116.
- 28 N. K. Dutta, M. Y. Truong, S. Mayavan, N. Roy Choudhury, C. M. Elvin, M. Kim, R. Knott, K. M. Nairn and A. J. Hill, *Angew. Chem.*, 2011, **123**, 4520–4523.
- 29 F. G. Quiroz, N. K. Li, S. Roberts, P. Weber, M. Dzuricky, I. Weitzhandler, Y. G. Yingling and A. Chilkoti, *Sci. Adv.*, 2019, **5**, eaax5177.
- 30 F. G. Quiroz and A. Chilkoti, *Nat. Mater.*, 2015, **14**, 1164.
- 31 A. S. Holehouse and R. V. Pappu, *Nat. Mater.*, 2015, **14**, 1083.
- 32 S. Da Vela, F. Roosen-Runge, M. W. A. Skoda, R. M. J. Jacobs, T. Seydel, H. Frielinghaus, M. Sztucki, R. Schweins, F. Zhang and F. Schreiber, *J. Phys. Chem. B*, 2017, **121**, 5759–5769.
- 33 F. Platten, J. Hansen, D. Wagner and S. U. Egelhaaf, *J. Phys. Chem. Lett.*, 2016, **7**, 4008–4014.
- 34 A. C. Dumetz, A. M. Chockla, E. W. Kaler and A. M. Lenhoff, *Biophys. J.*, 2008, **94**, 570–583.
- 35 T. Gibaud and P. Schurtenberger, *J. Phys.: Condens. Matter*, 2009, **21**, 322201.
- 36 F. Zhang, G. Zoicher, A. Sauter, T. Stehle and F. Schreiber, *J. Appl. Crystallogr.*, 2011, **44**, 755–762.
- 37 S. Da Vela, M. K. Braun, A. Dörr, A. Greco, J. Möller, Z. Fu, F. Zhang and F. Schreiber, *Soft Matter*, 2016, **12**, 9334–9341.
- 38 O. Matsarskaia, S. Da Vela, A. Mariani, Z. Fu, F. Zhang and F. Schreiber, *J. Phys. Chem. B*, 2019, **123**, 1913–1919.
- 39 T. Narayanan, M. Sztucki, P. Van Vaerenbergh, J. Leonardon, J. Gorini, L. Claustre, F. Sever, J. Morse and P. Boesecke, *J. Appl. Crystallogr.*, 2018, **51**, 1511–1524.
- 40 F. Zhang, M. W. A. Skoda, R. M. J. Jacobs, S. Zorn, R. A. Martin, C. M. Martin, G. F. Clark, S. Weggler, A. Hildebrandt, O. Kohlbacher and F. Schreiber, *Phys. Rev. Lett.*, 2008, **101**, 148101.
- 41 M. K. Braun, A. Sauter, O. Matsarskaia, M. Wolf, F. Roosen-Runge, M. Sztucki, R. Roth, F. Zhang and F. Schreiber, *J. Phys. Chem. B*, 2018, **122**, 11978–11985.
- 42 O. Matsarskaia, F. Roosen-Runge, G. Lotze, J. Möller, A. Mariani, F. Zhang and F. Schreiber, *Phys. Chem. Chem. Phys.*, 2018, **20**, 27214–27225.
- 43 O. Glatter and O. Kratky, *Small angle X-ray scattering*, Academic Press, London, USA, Edition New York, 1982.
- 44 F. Zhang, F. Roosen-Runge, A. Sauter, M. Wolf, R. M. J. Jacobs and F. Schreiber, *Pure Appl. Chem.*, 2014, **86**, 191–202.
- 45 M. K. Braun, M. Wolf, O. Matsarskaia, S. Da Vela, F. Roosen-Runge, M. Sztucki, R. Roth, F. Zhang and F. Schreiber, *J. Phys. Chem. B*, 2017, **121**, 1731–1739.
- 46 A. Shirayayev, D. L. Pagan, J. D. Gunton, D. S. Rhen, A. Saxena and T. Lookman, *J. Chem. Phys.*, 2005, **122**, 234911.
- 47 J. Li, R. Rajagopalan and J. Jiang, *J. Chem. Phys.*, 2008, **128**, 05B621.
- 48 F. Roosen-Runge, F. Zhang, F. Schreiber and R. Roth, *Sci. Rep.*, 2014, **4**, 7016.
- 49 G. A. Jeffrey, *Hydrogen Bonding in Biological Structures*, Springer-Verlag, Berlin, Heidelberg, 1991.
- 50 K. V. Ragnarsdottir, E. H. Oelkers, D. M. Sherman and C. R. Collins, *Chem. Geol.*, 1998, **151**, 29–39.
- 51 P. Lindqvist-Reis, K. Lambale, S. Pattanaik, I. Persson and M. Sandström, *J. Phys. Chem. B*, 2000, **104**, 402–408.
- 52 R. Maier, A. Sauter, G. Zoicher, S. Da Vela, O. Matsarskaia, R. Schweins, M. Sztucki, F. Zhang, T. Stehle and F. Schreiber, 2020, in preperation.
- 53 S. Moelbert and P. De Los Rios, *Macromolecules*, 2003, **36**, 5845–5853.